Performance Analysis of Millimeter Wave NOMA Networks with Beam Misalignment

Yong Zhou*, Vincent W.S. Wong*, and Robert Schober†
*Department of Electrical and Computer Engineering, The University of British Columbia, Vancouver, Canada
†Institute for Digital Communications, Friedrich-Alexander-University (FAU), Erlangen, Germany
e-mail: *{zhou, vincentw}@ece.ubc.ca, †robert.schober@fau.de

***Abstract*—Non-orthogonal multiple access (NOMA) and millimeter wave (mmWave) are two key enabling technologies for the fifth generation (5G) wireless networks. In this paper, we develop a general performance analysis framework for mmWave-NOMA networks with spatially random users taking into account link blockage and directional beamforming. To facilitate NOMA transmission in mmWave networks, we propose an angle-based user pairing strategy. Specifically, the base station first randomly selects one user and then pairs it with the line-of-sight user that has the minimum relative angle difference. NOMA is enabled when the beamwidth of the main lobe created by directional beamforming is not smaller than the angle difference between the paired NOMA users. Tools from stochastic geometry are utilized to derive the coverage probability and the sum rate of the proposed NOMA scheme, where beam misalignment at both the base station and the users is taken into account. Simulations validate the performance analysis and show that the proposed NOMA scheme achieves a larger coverage probability and a higher sum rate than conventional NOMA with distance-based user pairing and orthogonal multiple access.**

I. Introduction

Non-orthogonal multiple access (NOMA) [1], [2] has the potential to enhance the spectral efficiency of the fifth generation (5G) wireless networks, which is vital for meeting the rapidly increasing traffic demand. Different from conventional orthogonal multiple access (OMA), NOMA applies superposition coding at the transmitter side and successive interference cancellation (SIC) at the receiver side. With NOMA, multiple users can be simultaneously served by a base station in the same frequency band.

NOMA has recently received considerable research interest [2]–[6]. System-level performance evaluations in [2] show that transmit power allocation and user pairing are two important design aspects of NOMA. The authors in [3] propose an optimal power allocation policy to maximize the weighted sum rate of multicarrier NOMA systems. The impact of user pairing on the outage probability and the sum rate of NOMA is studied in [4]. The performance gain of NOMA over OMA under unsaturated traffic conditions is studied in [5].

Millimeter wave (mmWave) is another key enabling technology for 5G wireless networks [7]. The signals at mmWave frequencies (i.e., 30-300 GHz) are more sensitive to blockage effects compared to sub-6 GHz frequencies. The 3rd Generation Partnership Project (3GPP) reported stark differences in the propagation characteristics between line-of-sight (LOS) and non-line-of-sight (NLOS) links [8]. Due to the short wavelength of mmWave signals, antenna arrays can be deployed at the base station and the devices to implement beamforming. By using a sectored model to approximate the beamforming pattern, the authors in [9] analyze the coverage and rate of mmWave networks.

The coexistence of NOMA and mmWave has recently been studied in [10]–[12]. The authors in [10] apply random beamforming in mmWave-NOMA networks to reduce the channel estimation overhead. Taking into account hardware constraints, the application of finite resolution analog beamforming in mmWave-NOMA networks is studied in [11]. The authors in [12] analyze the capacity of mmWave-NOMA networks in both noise-limited and interference-limited scenarios. However, in practical implementations, beam misalignment at the base station and the users is inevitable [13]. This can reduce the probability that the paired NOMA users are covered by the main lobe created by directional beamforming and in turn degrade the network performance. This effect was not considered in [10]–[12]. Hence, a new user pairing strategy and the corresponding performance analysis framework taking into account beam misalignment are needed for mmWave-NOMA networks.

In this paper, we consider a downlink mmWave-NOMA network with spatially random users. As the link blockage model is distance-dependent, the spatial locations of the LOS and NLOS users are modeled as independent inhomogeneous Poisson point processes (PPPs). We take into account directional beamforming and beam misalignment at both the base station and the paired NOMA users. To facilitate NOMA transmission in mmWave networks, we propose an angle-based user pairing strategy. The base station first randomly selects one user and then pairs it with the LOS user that has the minimum relative angle difference. The proposed strategy increases the probability that the paired NOMA users are covered by the main lobe of the base station, even in the presence of beam misalignment. The main contributions of this paper are summarized as follows:

- We develop a general and tractable performance analysis framework for mmWave-NOMA networks with spatially random users taking into account link blockage, directional beamforming, beam misalignment, and user pairing.
- We derive the distributions of the involved random variables, including the distances of the LOS and NLOS users, the angle difference between the paired NOMA users, and the total directivity gains between the base station and both users. Based on these results, we derive the coverage probability and

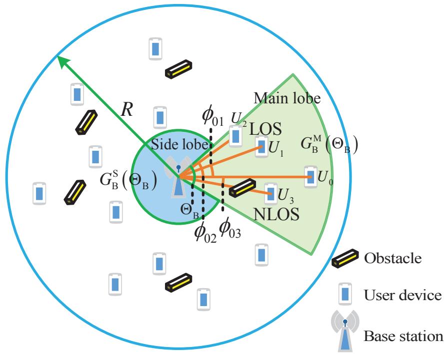

Fig. 1: Network topology for the considered downlink mmWave network. The absolute value of the angle difference between users U_0 and U_i is denoted as ϕ_{0i}. We pair the LOS user that has the minimum angle difference to the typical user. For example, user U_1 is selected as the paired NOMA user for typical user U_0, as user U_3 is an NLOS user and $\phi_{01} < \phi_{02}$.

the sum rate of the proposed NOMA scheme.

- Simulations validate the performance analysis and show that the proposed NOMA scheme outperforms conventional NOMA with distance-based user pairing and OMA in terms of the coverage probability and the sum rate.

The remainder of this paper is organized as follows. In Section II, we describe the system model for mmWave-NOMA networks. The coverage probability and sum rate are analyzed in Section III. Numerical and simulation results are presented in Section IV. Finally, Section V concludes this paper.

II. System Model

A. Network Topology

Consider downlink NOMA transmission in an mmWave cellular network, which consists of one base station and multiple spatially random users, as shown in Fig. 1. The base station is located at the center of a circular network coverage area with radius R. The locations of the users are assumed to follow a homogeneous PPP, denoted as Φ, with density λ, which represents the average number of users per unit area.

As mmWave links are vulnerable to blockage effects, it is necessary to model both LOS and NLOS path loss characteristics. For outdoor transmission, a link can be either LOS or NLOS. The blockages of different links are assumed to be independent from each other, as in [9], [10]. The probability that a link of length r is LOS is modeled as $p(r) = \exp\left(-r/\eta\right)$ [9], where η denotes the average LOS range. According to [14], the path losses of the LOS and NLOS links can be written as $\ell_{\mathrm{L}}(r) = C_{\mathrm{L}} r^{-\beta_{\mathrm{L}}}$ and $\ell_{\mathrm{N}}(r) = C_{\mathrm{N}} r^{-\beta_{\mathrm{N}}}$, respectively, where C_{L} and C_{N} are the intercepts of the LOS and NLOS path loss formulas, respectively, and β_{L} and β_{N} are the path loss exponents of the LOS and NLOS links, respectively. The blockage of a link is distance-dependent, and thus, both the LOS and NLOS users are not homogeneously distributed. The homogeneous PPP Φ can be divided into two independent inhomogeneous PPPs, denoted as Φ_{L} and $\Phi_{\mathrm{N}} = \Phi \setminus \Phi_{\mathrm{L}}$, which comprise the locations of the LOS and NLOS users, respectively. The densities of PPPs Φ_{L} and Φ_{N} are given by $\lambda p(r)$ and $\lambda\left(1 - p(r)\right)$, respectively. Due to the limited scattering at mmWave frequencies, each link is assumed to suffer from independent quasi-static Nakagami-m fading [9], [10]. The parameters of the Nakagami-m fading for the LOS and NLOS links are denoted as N_{L} and N_{N}, respectively, and are assumed to be positive integers for simplicity. Hence, the channel fading coefficient between the base station and user U_i, denoted as $|h_i|^2$, is a normalized Gamma random variable.

B. Directional Beamforming

Due to the short wavelength of mmWave signals, antenna arrays are deployed at both the base station and users to perform directional beamforming. For tractability of the performance analysis, we consider a sectored-pattern antenna model, as show in Fig. 1. Such a model is also adopted in other recent studies [9], [15], [16]. The directional antenna gain is

$$G_{\mathrm{a}}(\Theta_{\mathrm{a}},\phi) = \begin{cases} G_{\mathrm{a}}^{\mathrm{M}}(\Theta_{\mathrm{a}}) = \frac{2\pi}{\Theta_{\mathrm{a}}}\frac{\gamma_{\mathrm{a}}}{\gamma_{\mathrm{a}}+1}, & \text{if } |\phi| \le \frac{1}{2}\Theta_{\mathrm{a}}, \\ G_{\mathrm{a}}^{\mathrm{S}}(\Theta_{\mathrm{a}}) = \frac{2\pi}{2\pi-\Theta_{\mathrm{a}}}\frac{1}{\gamma_{\mathrm{a}}+1}, & \text{if } |\phi| > \frac{1}{2}\Theta_{\mathrm{a}}, \end{cases} \tag{1}$$

where $\mathrm{a} \in \{\mathrm{B},\mathrm{U}\}$ represents either the base station (B) or a user (U), ϕ denotes the angle off the boresight direction, Θ_{a} denotes the beamwidth of the main lobe, $G_{\mathrm{a}}^{\mathrm{M}}(\Theta_{\mathrm{a}})$ and $G_{\mathrm{a}}^{\mathrm{S}}(\Theta_{\mathrm{a}})$ denote the antenna gains of the main lobe and the side lobe, respectively, $\gamma_{\mathrm{a}} = \frac{2\pi}{C_0(2\pi-\Theta_{\mathrm{a}})}$ is the forward-to-backward power ratio, and C_0 is a constant. The sectored-pattern antenna model in (1) ensures that the total transmit power is constant, i.e., $\int_0^{2\pi} G_{\mathrm{a}}(\Theta_{\mathrm{a}},\phi)\mathrm{d}\phi = G_{\mathrm{a}}^{\mathrm{M}}(\Theta_{\mathrm{a}})\frac{\Theta_{\mathrm{a}}}{2\pi} + G_{\mathrm{a}}^{\mathrm{S}}(\Theta_{\mathrm{a}})\frac{2\pi-\Theta_{\mathrm{a}}}{2\pi} = 1$. The base station and the users can adjust their beam orientation to cover the intended receiver/transmitter in the main lobe.

We denote the additive beamsteering errors of the base station and user U_i as Δ_{B} and Δ_{U_i}, respectively. We assume that Δ_{B} and $\{\Delta_{\mathrm{U}_i}, z_i \in \Phi\}$ are independent and identically distributed, where z_i denotes the location of user U_i. We assume that the beamsteering errors follow a Gaussian distribution with zero mean and variance $\sigma_{\mathrm{a}}^2, \mathrm{a} \in \{\mathrm{B},\mathrm{U}\}$. Hence, the cumulative distribution function (CDF) of the beamsteering error is $F_{\Delta_{\mathrm{a}}}(x) = \frac{1}{2}\left(1 + \mathrm{erf}\left(\frac{x}{\sigma_{\mathrm{a}}\sqrt{2}}\right)\right), \mathrm{a} \in \{\mathrm{B},\mathrm{U}\}$, where $\mathrm{erf}(\cdot)$ is the error function.

C. NOMA Scheme for mmWave Networks

We consider the case where two users are paired for NOMA transmission, which has been also included in the 3GPP standard [17]. For fairness, the base station first selects one user at random. This user is referred to as the typical user and denoted as U_0. To facilitate NOMA transmission in mmWave networks, we propose an angle-based user pairing strategy. Specifically, the user paired with the typical user U_0 is denoted as U_{p} and is selected based on the following criterion

$$z_{\mathrm{p}} = \begin{cases} \arg \min\limits_{z_i \in \Phi_{\mathrm{L}} \setminus \{z_0\}} \{\phi_{0i}\}, & \text{if user } U_0 \text{ is LOS}, \\ \arg \min\limits_{z_i \in \Phi_{\mathrm{L}}} \{\phi_{0i}\}, & \text{if user } U_0 \text{ is NLOS}, \end{cases} \tag{2}$$

where z_{p} is the location of the paired NOMA user U_{p}, ϕ_i is the angle of user U_i with respect to the base station, and $\phi_{0i} = |\phi_0 - \phi_i|$ is the absolute value of the angle difference between angles ϕ_0 and ϕ_i. The proposed user pairing strategy selects the LOS user that has the minimum angle difference (i.e., $\phi_{0\mathrm{p}}$) to the typical user. Hence, the angle information

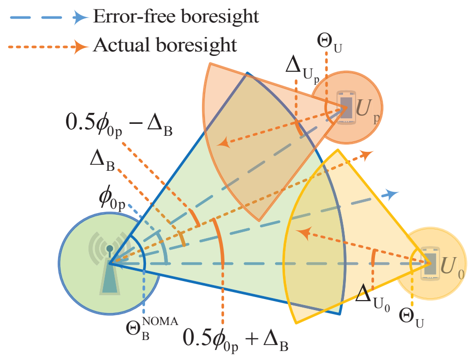

Fig. 2: Directional beamforming of the base station and both NOMA users with beamsteering errors. The error-free boresight direction of the base station has the same angle difference (i.e., $0.5\phi_{0\rm p}$) to typical user U_0 and paired NOMA user $U_{\rm p}$. However, due to beam misalignment, there is a beamsteering error (i.e., $\Delta_{\rm B}$) between the actual and the error-free boresight directions.

of each LOS user has to be known at the base station. With this angle-based user pairing strategy, it is highly likely that both NOMA users are covered by the main lobe of the base station and, as a consequence, can exploit the array gain, even in the presence of beam misalignment. On the other hand, with the conventional distance-based user pairing strategy [18], which was developed for omni-directional transmission, beam misalignment may lead to large performance degradation in mmWave networks with directional beamforming.

The base station performs NOMA and simultaneously serves users U_0 and $U_{\rm p}$ if $\phi_{0\rm p} \le \Theta_{\rm B}^{\rm NOMA}$, where $\Theta_{\rm B}^{\rm NOMA}$ is the beamwidth of the main lobe of the base station when NOMA is enabled. On the other hand, if $\phi_{0\rm p} > \Theta_{\rm B}^{\rm NOMA}$, i.e., the base station cannot cover both NOMA users in the main lobe even without beam misalignment, the base station serves users U_0 and $U_{\rm p}$ using OMA with beamwidth $\Theta_{\rm B}^{\rm OMA}$. The beamwidth of the main lobe at the base station required for NOMA transmission is not smaller than that for OMA transmission, i.e., $\Theta_{\rm B}^{\rm NOMA} \ge \Theta_{\rm B}^{\rm OMA}$, as NOMA needs to cover two users in the main lobe instead of only one.

We denote the power allocation coefficients for users U_0 and $U_{\rm p}$ as α_0 and $\alpha_{\rm p}$, respectively, with $\alpha_0 > \alpha_{\rm p}$ and $\alpha_0^2+\alpha_{\rm p}^2 = 1$. For NOMA transmission (i.e., $\phi_{0\rm p} \le \Theta_{\rm B}^{\rm NOMA}$), user U_0 is allocated a higher transmit power and decodes its own signal with the signal-to-interference-plus-noise ratio (SINR)

$$\gamma_{0|\rm p} = \frac{\alpha_0^2 P_{\rm B} \left|h_0\right|^2 \mathcal{D}_0^{\rm NOMA} \ell_\nu(r_0)}{\alpha_{\rm p}^2 P_{\rm B} \left|h_0\right|^2 \mathcal{D}_0^{\rm NOMA} \ell_\nu(r_0) + \sigma^2}, \tag{3}$$

where $\nu \in \{\rm L, N\}$ represents either LOS (L) or NLOS (N), $P_{\rm B}$ denotes the total transmit power of the base station, $\mathcal{D}_0^{\rm NOMA}$ denotes the total directivity gain between the base station and user U_0 when NOMA is enabled, r_0 denotes the distance between the base station and user U_0, and σ^2 denotes the power of additive white Gaussian noise (AWGN).

To reduce the adverse effect of beam misalignment on the coverage of the paired NOMA users in the main lobe, the base station adjusts its beam orientation so that its error-free boresight direction has the same angle difference (i.e., $\frac{1}{2}\phi_{0\rm p}$) with respect to users U_0 and $U_{\rm p}$, as shown in Fig. 2. However, due to beam misalignment, there is a beamsteering error (i.e., $\Delta_{\rm B}$) between the actual and error-free boresight directions. As a result, the total directivity gain between the base station and user U_0 for NOMA transmission is given by

$$\mathcal{D}_0^{\rm NOMA} = G_{\rm B}\left(\Theta_{\rm B}^{\rm NOMA}, 0.5\phi_{0\rm p} + \Delta_{\rm B}\right) G_{\rm U}\left(\Theta_{\rm U}, \Delta_{\rm U_0}\right), \tag{4}$$

where $\Theta_{\rm U}$ denotes the beamwidth of the main lobe at the user.

On the other hand, the paired NOMA user first decodes the signal intended for user U_0 with SINR

$$\gamma_{0\to\rm p} = \frac{\alpha_0^2 P_{\rm B} \left|h_{\rm p}\right|^2 \mathcal{D}_{\rm p}^{\rm NOMA} \ell_{\rm L}(r_{\rm p})}{\alpha_{\rm p}^2 P_{\rm B} \left|h_{\rm p}\right|^2 \mathcal{D}_{\rm p}^{\rm NOMA} \ell_{\rm L}(r_{\rm p}) + \sigma^2}, \tag{5}$$

where $\mathcal{D}_{\rm p}^{\rm NOMA}$ denotes the total directivity gain between the base station and the paired NOMA user $U_{\rm p}$ when NOMA is enabled. Similar to (4), we have

$$\mathcal{D}_{\rm p}^{\rm NOMA} = G_{\rm B}\left(\Theta_{\rm B}^{\rm NOMA}, 0.5\phi_{0\rm p} - \Delta_{\rm B}\right) G_{\rm U}\left(\Theta_{\rm U}, \Delta_{\rm U_p}\right). \tag{6}$$

If user $U_{\rm p}$ can successfully decode the signal intended for user U_0, then user $U_{\rm p}$ performs SIC and decodes its own signal with the following signal-to-noise ratio (SNR)

$$\gamma_{\rm p} = \alpha_{\rm p}^2 P_{\rm B} \left|h_{\rm p}\right|^2 \mathcal{D}_{\rm p}^{\rm NOMA} \ell_{\rm L}(r_{\rm p}) / \sigma^2. \tag{7}$$

Otherwise, user $U_{\rm p}$ cannot perform SIC and decode its signal, i.e., an outage occurs.

When a second NOMA user for pairing does not exist or the angle difference is $\phi_{0\rm p} \ge \Theta_{\rm B}^{\rm NOMA}$, the base station cannot cover two NOMA users in the main lobe, even without beam misalignment. Thereby, the base station serves users U_0 and $U_{\rm p}$ using OMA with beamwidth $\Theta_{\rm B}^{\rm OMA}$ of the main lobe. The received SNR observed at user $U_j, j \in \{0, \rm p\}$, is given by

$$\gamma_{j,\nu}^{\rm OMA} = P_{\rm B} \left|h_j\right|^2 \mathcal{D}_j^{\rm OMA} \ell_\nu(r_j) / \sigma^2, \tag{8}$$

where $\nu \in \{\rm L, N\}$, and $\mathcal{D}_j^{\rm OMA}$ is the total directivity gain between the base station and user U_j when OMA is enabled. For OMA, the base station adjusts its beam orientation so that its error-free boresight direction is aligned with the vector from the base station to user U_j. The total directivity gain between the base station and user U_j for OMA is

$$\mathcal{D}_j^{\rm OMA} = G_{\rm B}\left(\Theta_{\rm B}^{\rm OMA}, \Delta_{\rm B}\right) G_{\rm U}\left(\Theta_{\rm U}, \Delta_{\rm U_j}\right). \tag{9}$$

The SINRs and the total directivity gains given in (3) – (9) are all random variables, due to the randomness of the small-scale fading, the angle difference, the beamsteering errors, the user distances, and the link blockage status.

III. Coverage Probability and Sum Rate Analysis

A. Some Useful Probability Density Functions

To calculate the coverage probability, we first need to derive the probability density functions (PDFs) of the involved random variables, including the user distance, angle difference, and total directivity gain. The corresponding results are given in the following lemmas.

Lemma 1. *The PDF of the distance between the base station and a randomly selected LOS user is given by*

$$f_{\rm L}(r) = (r/\rho) \exp\left(-r/\eta\right), \qquad 0 \le r \le R, \tag{10}$$

where $\rho = \eta^2 \left(1 - \exp\left(-R/\eta\right)\left(1 + R/\eta\right)\right)$.

Similarly, the PDF of the distance between the base station and a randomly selected NLOS user is given by

$$f_{\rm N}(r) = \frac{2r}{R^2 - 2\rho}\left(1 - \exp\left(-\frac{r}{\eta}\right)\right),\ 0 \le r \le R. \quad (11)$$

Proof. Please refer to Appendix A. □

As the spatial locations of the LOS and NLOS users form inhomogeneous PPPs $\Phi_{\rm L}$ and $\Phi_{\rm N}$ with densities $\lambda p(r)$ and $\lambda(1 - p(r))$, respectively, the probability mass functions (PMFs) of the number of LOS and NLOS users in the network coverage area can, respectively, be expressed as

$$\Psi_{\rm L}(k_{\rm L}) = \left(\lambda 2\pi\rho\right)^{k_{\rm L}} \exp\left(-\lambda 2\pi\rho\right)/k_{\rm L}!, \quad (12)$$

$$\Psi_{\rm N}\left(k_{\rm N}\right) = \left(\lambda\pi\left(R^2 - 2\rho\right)\right)^{k_{\rm N}} \exp\left(-\lambda\pi\left(R^2 - 2\rho\right)\right)/k_{\rm N}!, \quad (13)$$

where $k_{\rm L}$ and $k_{\rm N}$ denote the number of the LOS and NLOS users in the network coverage area, respectively.

Lemma 2. *Based on the user pairing strategy in (2), the PDF of the angle difference between the typical user and the paired NOMA user, $\phi_{0\rm p}$, when there are $k_{\rm L}$ LOS users, is given by*

$$f_{\phi_{0\rm p}}(\phi) = \begin{cases} \frac{k_{\rm L}-1}{\pi}\left(\frac{2\pi-\phi}{2\pi}\right)^{2k_{\rm L}-3}, & \text{if } U_0 \text{ is LOS,} \\ \frac{k_{\rm L}}{\pi}\left(\frac{2\pi-\phi}{2\pi}\right)^{2k_{\rm L}-1}, & \text{if } U_0 \text{ is NLOS.} \end{cases} \quad (14)$$

Proof. Please refer to Appendix B. □

Lemma 3. *Given the angle difference $\phi_{0\rm p}$ between the typical user and the paired NOMA user, the PMFs of the total directivity gains $\mathcal{D}_0^{\rm NOMA}$ and $\mathcal{D}_{\rm p}^{\rm NOMA}$ when NOMA is enabled can, respectively, be expressed as*

$$\mathbb{P}\left(\mathcal{D}_0^{\rm NOMA} = c_i\right) = d_i\left(\phi_{0\rm p}\right), \quad \text{for } i = \{1,2,3,4\}, \quad (15)$$

$$\mathbb{P}\left(\mathcal{D}_{\rm p}^{\rm NOMA} = c_i\right) = v_i\left(\phi_{0\rm p}\right), \quad \text{for } i = \{1,2,3,4\}, \quad (16)$$

where $g(\phi_{0\rm p}) = \frac{1}{2}\left(\operatorname{erf}\left(\frac{\Theta_{\rm B}^{\rm NOMA}-\phi_{0\rm p}}{2\sqrt{2}\sigma_{\rm B}}\right) - \operatorname{erf}\left(-\frac{\Theta_{\rm B}^{\rm NOMA}+\phi_{0\rm p}}{2\sqrt{2}\sigma_{\rm B}}\right)\right)$, $s(\phi_{0\rm p}) = \frac{1}{2}\left(\operatorname{erf}\left(\frac{\Theta_{\rm B}^{\rm NOMA}+\phi_{0\rm p}}{2\sqrt{2}\sigma_{\rm B}}\right) - \operatorname{erf}\left(-\frac{\Theta_{\rm B}^{\rm NOMA}-\phi_{0\rm p}}{2\sqrt{2}\sigma_{\rm B}}\right)\right)$, $y = \frac{1}{2}\left(\operatorname{erf}\left(\frac{\Theta_{\rm U}}{2\sqrt{2}\sigma_{\rm U}}\right) - \operatorname{erf}\left(-\frac{\Theta_{\rm U}}{2\sqrt{2}\sigma_{\rm U}}\right)\right)$, *and*

$$c_1 = G_{\rm B}^{\rm M}(\Theta_{\rm B}^{\rm NOMA})G_{\rm U}^{\rm M}(\Theta_{\rm U}),\ c_2 = G_{\rm B}^{\rm M}(\Theta_{\rm B}^{\rm NOMA})G_{\rm U}^{\rm S}(\Theta_{\rm U}),$$
$$c_3 = G_{\rm B}^{\rm S}(\Theta_{\rm B}^{\rm NOMA})G_{\rm U}^{\rm M}(\Theta_{\rm U}),\ c_4 = G_{\rm B}^{\rm S}(\Theta_{\rm B}^{\rm NOMA})G_{\rm U}^{\rm S}(\Theta_{\rm U}),$$
$$d_1(\phi_{0\rm p}) = g\left(\phi_{0\rm p}\right)y, \qquad d_2(\phi_{0\rm p}) = g\left(\phi_{0\rm p}\right)(1-y),$$
$$d_3(\phi_{0\rm p}) = (1 - g\left(\phi_{0\rm p}\right))y, d_4(\phi_{0\rm p}) = (1 - g\left(\phi_{0\rm p}\right))(1-y),$$
$$v_1(\phi_{0\rm p}) = s\left(\phi_{0\rm p}\right)y, \qquad v_2(\phi_{0\rm p}) = s\left(\phi_{0\rm p}\right)(1-y),$$
$$v_3(\phi_{0\rm p}) = (1 - s\left(\phi_{0\rm p}\right))y, v_4(\phi_{0\rm p}) = (1 - s\left(\phi_{0\rm p}\right))(1-y).$$

Proof. Please refer to Appendix C. □

Whether NOMA or OMA is enabled depends on angle difference $\phi_{0\rm p}$. The coverage probability is defined as the probability that a user can successfully decode the signal transmitted by the base station with a certain target data rate. We denote the target data rates of users U_0 and $U_{\rm p}$ by R_0 and $R_{\rm p}$, respectively. The coverage probabilities for both NOMA and OMA transmission in the proposed NOMA scheme are derived in the following two subsections.

B. Coverage Probability for NOMA Transmission

When both NOMA users are LOS and $\phi_{0\rm p} \le \Theta_{\rm B}^{\rm NOMA}$, the coverage probability of user $U_j, j \in \{0, \rm p\}$, is given by

$$P_j^{\rm cov,I} = \sum_{k_{\rm L}=2}^{\infty}\sum_{k_{\rm N}=0}^{\infty} \frac{k_{\rm L}}{k_{\rm L}+k_{\rm N}}\Psi_{\rm L}(k_{\rm L})\Psi_{\rm N}(k_{\rm N})Q_{j,\rm L}, \quad (17)$$

where $\sum_{k_{\rm L}=2}^{\infty}\sum_{k_{\rm N}=0}^{\infty}\frac{k_{\rm L}}{k_{\rm L}+k_{\rm N}}\Psi_{\rm L}(k_{\rm L})\Psi_{\rm N}(k_{\rm N})$ is the probability that there are at least two LOS users and user U_0 is LOS, $Q_{0,\rm L} = \mathbb{P}\left(\gamma_{0|\rm p} \ge T_0, \phi_{0\rm p} \le \Theta_{\rm B}^{\rm NOMA}\right)$ is the probability that user U_0 can successfully decode its own signal when NOMA is enabled, $Q_{\rm p,L} = \mathbb{P}\left(\gamma_{0\to\rm p} \ge T_0, \gamma_{\rm p} \ge T_{\rm p}, \phi_{0\rm p} \le \Theta_{\rm B}^{\rm NOMA}\right)$ is the probability that user $U_{\rm p}$ can successfully perform SIC and decode its own signal when NOMA is enabled, $T_0 = 2^{R_0} - 1$, and $T_{\rm p} = 2^{R_{\rm p}} - 1$.

Proposition 1. *Given that there are $k_{\rm L}$ LOS users and $k_{\rm N}$ NLOS users, $Q_{0,\rm L}$ and $Q_{\rm p,L}$ are, respectively, given by*

$$Q_{0,\rm L} = \sum_{n=0}^{N_{\rm L}-1}\frac{(N_{\rm L}\xi_1)^n}{n!}\sum_{i=1}^{4}\int_0^{\Theta_{\rm B}^{\rm NOMA}} d_i(\phi_{0\rm p})f_{\phi_{0\rm p}}(\phi_{0\rm p})\mathrm{d}\phi_{0\rm p} \times \int_0^R \left(\frac{r_0^{\beta_{\rm L}}}{c_i C_{\rm L}}\right)^n \exp\left(-\frac{N_{\rm L}\xi_1 r_0^{\beta_{\rm L}}}{c_i C_{\rm L}}\right) f_{\rm L}(r_0)\mathrm{d}r_0, \quad (18)$$

$$Q_{\rm p,L} = \sum_{n=0}^{N_{\rm L}-1}\frac{(N_{\rm L}\xi_2)^n}{n!}\sum_{i=1}^{4}\int_0^{\Theta_{\rm B}^{\rm NOMA}} v_i(\phi_{0\rm p})f_{\phi_{0\rm p}}(\phi_{0\rm p})\mathrm{d}\phi_{0\rm p} \times \int_0^R \left(\frac{r_{\rm p}^{\beta_{\rm L}}}{c_i C_{\rm L}}\right)^n \exp\left(-\frac{N_{\rm L}\xi_2 r_{\rm p}^{\beta_{\rm L}}}{c_i C_{\rm L}}\right) f_{\rm L}(r_{\rm p})\mathrm{d}r_{\rm p}, \quad (19)$$

if $\alpha_0^2 > T_0\alpha_{\rm p}^2$, *otherwise* $Q_{0,\rm L} = 0$ *and* $Q_{\rm p,L} = 0$, *where* $\xi_1 = \frac{T_0\sigma^2}{(\alpha_0^2 - T_0\alpha_{\rm p}^2)P_{\rm B}}$ *and* $\xi_2 = \max\left\{\frac{T_0\sigma^2}{(\alpha_0^2 - T_0\alpha_{\rm p}^2)P_{\rm B}}, \frac{T_{\rm p}\sigma^2}{\alpha_{\rm p}^2 P_{\rm B}}\right\}$.

Proof. Please refer to Appendix D. □

Similarly, when the typical user is NLOS, the paired NOMA user is LOS, and $\phi_{0\rm p} \le \Theta_{\rm B}^{\rm NOMA}$, the coverage probability of users U_0 and $U_{\rm p}$ can be expressed as

$$P_0^{\rm cov,II} = \sum_{k_{\rm L}=2}^{\infty}\sum_{k_{\rm N}=0}^{\infty}\frac{k_{\rm L}}{k_{\rm L}+k_{\rm N}}\Psi_{\rm L}(k_{\rm L})\Psi_{\rm N}(k_{\rm N})Q_{0,\rm N}, \quad (20)$$

and $P_{\rm p}^{\rm cov,II} = P_{\rm p}^{\rm cov,I}$, respectively, where $Q_{0,\rm N}$ is given by (18) after replacing $N_{\rm L}$, $C_{\rm L}$, $\beta_{\rm L}$, and $f_{\rm L}(r_0)$ with $N_{\rm N}$, $C_{\rm N}$, $\beta_{\rm N}$, and $f_{\rm N}(r_0)$, respectively.

C. Coverage Probability for OMA Transmission

When a second NOMA user for pairing does not exist or $\phi_{0\rm p} > \Theta_{\rm B}^{\rm NOMA}$, OMA is enabled. The following lemma gives the PMF of the total directivity gain $\mathcal{D}_j^{\rm OMA}$, $j \in \{0, \rm p\}$.

Lemma 4. *The PMF of the total directivity gain $\mathcal{D}_j^{\rm OMA}, j \in \{0, \rm p\}$, when OMA is enabled can be expressed as*

$$\mathbb{P}\left(\mathcal{D}_j^{\rm OMA} = l_i\right) = m_i, \qquad \text{for } i = \{1,2,3,4\}, \quad (21)$$

where $w = \frac{1}{2}\left(\operatorname{erf}\left(\frac{\Theta_{\rm B}^{\rm OMA}}{2\sqrt{2}\sigma_{\rm B}}\right) - \operatorname{erf}\left(-\frac{\Theta_{\rm B}^{\rm OMA}}{2\sqrt{2}\sigma_{\rm B}}\right)\right)$, *and*

$$l_1 = G_{\rm B}^{\rm M}(\Theta_{\rm B}^{\rm OMA})G_{\rm U}^{\rm M}(\Theta_{\rm U}), \quad l_2 = G_{\rm B}^{\rm M}(\Theta_{\rm B}^{\rm OMA})G_{\rm U}^{\rm S}(\Theta_{\rm U}),$$

$$l_3 = G_{\mathrm{B}}^{\mathrm{S}}(\Theta_{\mathrm{B}}^{\mathrm{OMA}}) G_{\mathrm{U}}^{\mathrm{M}}(\Theta_{\mathrm{U}}), \quad l_4 = G_{\mathrm{B}}^{\mathrm{S}}(\Theta_{\mathrm{B}}^{\mathrm{OMA}}) G_{\mathrm{U}}^{\mathrm{S}}(\Theta_{\mathrm{U}}),$$
$$m_1 = wy, \quad m_2 = w(1-y),$$
$$m_3 = (1-w)y, \quad m_4 = (1-w)(1-y). \tag{22}$$

Proof. The proof is similar to that of Lemma 3, and hence, it is omitted here. □

Based on Lemma 4, the complementary CDF (CCDF) of $\gamma_{j,\nu}^{\mathrm{OMA}}, j \in \{0, \mathrm{p}\}, \nu \in \{\mathrm{L}, \mathrm{N}\}$, defined in (8) is given by

$$\begin{aligned}
&\overline{F}_{\gamma_{j,\nu}^{\mathrm{OMA}}}(\gamma) \overset{(a)}{=} \mathbb{P}\left(|h_j|^2 P_{\mathrm{B}} \mathcal{D}_j^{\mathrm{OMA}} \ell_\nu(r_j)/\sigma^2 \geq \gamma\right) \\
&\overset{(b)}{=} \sum_{n=0}^{N_\nu-1} \frac{\left(N_\nu \gamma \sigma^2/P_{\mathrm{B}}\right)^n}{n!} \mathbb{E}_{\{\mathcal{D}_j^{\mathrm{OMA}}, r_j\}}\left[\frac{\exp\left(-\frac{N_\nu \gamma \sigma^2/P_{\mathrm{B}}}{\mathcal{D}_j^{\mathrm{OMA}} \ell_\nu(r_j)}\right)}{\left(\mathcal{D}_j^{\mathrm{OMA}} \ell_\nu(r_j)\right)^n}\right] \\
&\overset{(c)}{=} \sum_{n=0}^{N_\nu-1} \frac{\left(N_\nu \gamma \sigma^2/P_{\mathrm{B}}\right)^n}{n!} \sum_{i=1}^{4} m_i \\
&\quad \times \int_0^R \left(\frac{r_j^{\beta_\nu}}{l_i C_\nu}\right)^n \exp\left(-\frac{N_\nu \gamma \sigma^2 r_j^{\beta_\nu}}{P_{\mathrm{B}} l_i C_\nu}\right) f_\nu(r_j) \mathrm{d}r_j,
\end{aligned} \tag{23}$$

where (a) follows by substituting (8), (b) follows as $|h_j|^2$ is normalized Gamma distributed, and (c) follows from taking the expectation over $\mathcal{D}_j^{\mathrm{OMA}}$ and r_j.

When the typical user is LOS, its coverage probability is

$$\begin{aligned}
P_{\mathrm{OMA},0}^{\mathrm{cov,I}} &= \Psi_{\mathrm{L}}(1)\Psi_{\mathrm{N}}(0)\overline{F}_{\gamma_{0,\mathrm{L}}^{\mathrm{OMA}}}(T_0) \\
&+ \Psi_{\mathrm{L}}(1) \sum_{k_{\mathrm{N}}=1}^{\infty} \frac{\Psi_{\mathrm{N}}(k_{\mathrm{N}})}{1+k_{\mathrm{N}}} \overline{F}_{\gamma_{0,\mathrm{L}}^{\mathrm{OMA}}}(2T_0) \\
&+ \sum_{k_{\mathrm{L}}=2}^{\infty} \sum_{k_{\mathrm{N}}=0}^{\infty} \frac{k_{\mathrm{L}} \Psi_{\mathrm{L}}(k_{\mathrm{L}})}{k_{\mathrm{L}}+k_{\mathrm{N}}} \Psi_{\mathrm{N}}(k_{\mathrm{N}}) Q_1^{\mathrm{OMA}}(T_0),
\end{aligned} \tag{24}$$

where $Q_1^{\mathrm{OMA}}(T_0) = \mathbb{P}\left(\gamma_{0,\mathrm{L}}^{\mathrm{OMA}} \geq 2T_0, \phi_{0\mathrm{p}} > \Theta_{\mathrm{B}}^{\mathrm{NOMA}}\right) \overset{(a)}{=} \overline{F}_{\gamma_{0,\mathrm{L}}^{\mathrm{OMA}}}(2T_0) \left(\frac{2\pi - \Theta_{\mathrm{B}}^{\mathrm{NOMA}}}{2\pi}\right)^{2k_{\mathrm{L}}-2}$. Note that (a) follows from the independence of $\gamma_{0,\mathrm{L}}^{\mathrm{OMA}}$ and $\phi_{0\mathrm{p}}$. On the right hand side of (24), the first term is the coverage probability when there is one LOS user and no NLOS user. The second term is the coverage probability when user U_0 is the only LOS user. The third term represents the coverage probability when both users U_0 and U_{p} are LOS but $\phi_{0\mathrm{p}} > \Theta_{\mathrm{B}}^{\mathrm{NOMA}}$. When OMA is enabled, the base station transmits the signals to users U_0 and U_{p} in the first and second halves of a time slot, respectively.

When user U_0 is NLOS, its coverage probability is

$$\begin{aligned}
P_{\mathrm{OMA},0}^{\mathrm{cov,II}} &= \Psi_{\mathrm{L}}(0)\Psi_{\mathrm{N}}(1)\overline{F}_{\gamma_{0,\mathrm{N}}^{\mathrm{OMA}}}(T_0) \\
&+ \Psi_{\mathrm{L}}(0)\left(1 - \Psi_{\mathrm{N}}(0) - \Psi_{\mathrm{N}}(1)\right) \overline{F}_{\gamma_{0,\mathrm{N}}^{\mathrm{OMA}}}(2T_0) \\
&+ \sum_{k_{\mathrm{L}}=1}^{\infty} \sum_{k_{\mathrm{N}}=1}^{\infty} \frac{k_{\mathrm{N}} \Psi_{\mathrm{L}}(k_{\mathrm{L}})}{k_{\mathrm{L}}+k_{\mathrm{N}}} \Psi_{\mathrm{N}}(k_{\mathrm{N}}) Q_2^{\mathrm{OMA}},
\end{aligned} \tag{25}$$

where $Q_2^{\mathrm{OMA}} = \overline{F}_{\gamma_{0,\mathrm{N}}^{\mathrm{OMA}}}(2T_0)\left(2\pi - \Theta_{\mathrm{B}}^{\mathrm{NOMA}}\right)^{2k_{\mathrm{L}}} / (2\pi)^{2k_{\mathrm{L}}}$.

Similar to (24) and (25), when OMA is used, the coverage probability of user U_{p} is given by

$$\begin{aligned}
P_{\mathrm{OMA,p}}^{\mathrm{cov}} &= \Psi_{\mathrm{L}}(1) \sum_{k_{\mathrm{N}}=1}^{\infty} \frac{\Psi_{\mathrm{N}}(k_{\mathrm{N}})}{1+k_{\mathrm{N}}} \overline{F}_{\gamma_{\mathrm{p,N}}^{\mathrm{OMA}}}(2T_{\mathrm{p}}) \\
&+ \sum_{k_{\mathrm{L}}=2}^{\infty} \sum_{k_{\mathrm{N}}=0}^{\infty} \frac{k_{\mathrm{L}} \Psi_{\mathrm{L}}(k_{\mathrm{L}})}{k_{\mathrm{L}}+k_{\mathrm{N}}} \Psi_{\mathrm{N}}(k_{\mathrm{N}}) Q_1^{\mathrm{OMA}}(T_{\mathrm{p}}) \\
&+ \Psi_{\mathrm{L}}(0)\left(1 - \Psi_{\mathrm{N}}(0) - \Psi_{\mathrm{N}}(1)\right) \overline{F}_{\gamma_{\mathrm{p,N}}^{\mathrm{OMA}}}(2T_{\mathrm{p}}) \\
&+ \sum_{k_{\mathrm{L}}=1}^{\infty} \sum_{k_{\mathrm{N}}=1}^{\infty} \frac{k_{\mathrm{N}} \Psi_{\mathrm{L}}(k_{\mathrm{L}})}{k_{\mathrm{L}}+k_{\mathrm{N}}} \Psi_{\mathrm{N}}(k_{\mathrm{N}}) Q_3^{\mathrm{OMA}},
\end{aligned} \tag{26}$$

where $Q_3^{\mathrm{OMA}} = \overline{F}_{\gamma_{\mathrm{p,L}}^{\mathrm{OMA}}}(2T_{\mathrm{p}})\left(2\pi - \Theta_{\mathrm{B}}^{\mathrm{NOMA}}\right)^{2k_{\mathrm{L}}} / (2\pi)^{2k_{\mathrm{L}}}$.

D. Coverage Probability and Sum Rate

We present the main result in the following theorem.

Theorem 1. *The coverage probabilities of the typical user and the paired NOMA user of the proposed scheme in mmWave-NOMA networks with beam misalignment are*

$$P_0^{\mathrm{cov}} = P_0^{\mathrm{cov,I}} + P_0^{\mathrm{cov,II}} + P_{\mathrm{OMA},0}^{\mathrm{cov,I}} + P_{\mathrm{OMA},0}^{\mathrm{cov,II}}, \tag{27}$$
$$P_{\mathrm{p}}^{\mathrm{cov}} = P_{\mathrm{p}}^{\mathrm{cov,I}} + P_{\mathrm{p}}^{\mathrm{cov,II}} + P_{\mathrm{OMA,p}}^{\mathrm{cov}}. \tag{28}$$

The sum rate of the typical user and the paired NOMA user is given by $R_{\mathrm{sum}} = P_0^{\mathrm{cov}} R_0 + P_{\mathrm{p}}^{\mathrm{cov}} R_{\mathrm{p}}$.

Proof. By considering all cases discussed in Sections III-B and III-C, we directly obtain the coverage probabilities of both NOMA users and the sum rate. □

IV. Performance Evaluation

In this section, we present simulation and analytical results for the proposed NOMA scheme and compare them with results for conventional NOMA and OMA. For conventional NOMA, we adopt distance-based user pairing, where the base station pairs the typical user with the user that is closest to the base station. For a fair comparison, in OMA, the base station transmits the signals to the typical user and the paired NOMA user in the first and second halves of a time slot, respectively. In the simulations, we consider a circular network coverage area with radius $R = 200$ m. The noise power is -90 dBm. Unless specified otherwise, we set $\beta_{\mathrm{L}} = 2$, $\beta_{\mathrm{N}} = 2.9$, $C_{\mathrm{L}} = 2$, $C_{\mathrm{N}} = 1$, $N_{\mathrm{L}} = 3$, $N_{\mathrm{N}} = 2$, $\eta = 50$ m, $\alpha_0^2 = 0.9$, $\alpha_{\mathrm{p}}^2 = 0.1$, $C_0 = 0.1$, $\Theta_{\mathrm{B}}^{\mathrm{NOMA}} = \pi/3$, $\Theta_{\mathrm{B}}^{\mathrm{OMA}} = \pi/6$, $\Theta_{\mathrm{U}} = \pi/6$, $R_0 = 2$ bits per channel use (BPCU), and $R_{\mathrm{p}} = 8$ BPCU.

Fig. 3 shows the impact of the transmit power (i.e., P_{B}) and the beam misalignment on the sum rate. The simulation (Sim) results match well with the analytical (Ana) results, which validates our performance analysis. When P_{B} increases, the sum rates of all considered schemes increase, as the received signal power increases. The sum rates of all considered schemes decrease when the variance of the beamsteering errors increases. This is because the probability that a user is covered by the main lobe of the base station decreases when the values of σ_{B}^2 and σ_{U}^2 increase. Moreover, the sum rate achieved by the proposed NOMA scheme is larger than that achieved by conventional NOMA. This is because for the proposed user pairing strategy the paired NOMA users are covered by the main lobe of the base station with a higher probability compared to conventional distance-based user pairing.

Fig. 4 investigates the impact of the user density (λ) on the coverage probabilities of both NOMA users. As λ increases,

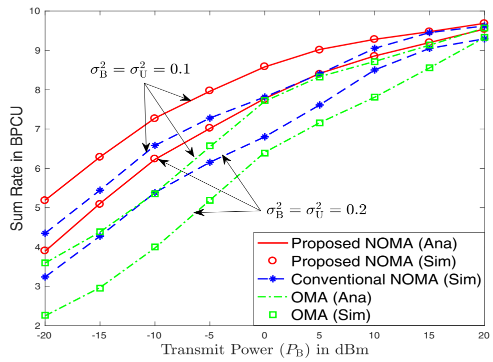

Fig. 3: Sum rate versus transmit power for different beamsteering error variances when $\lambda = 0.0002$ nodes/m^2.

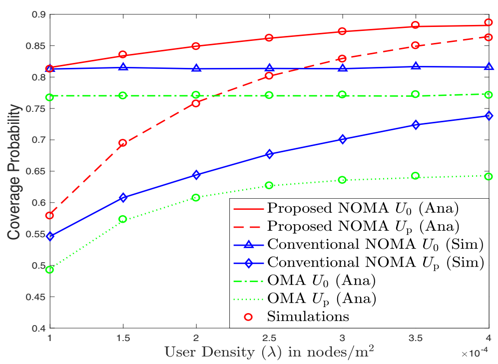

Fig. 4: Coverage probability versus user density when $P_{\mathrm{B}} = 0$ dBm and $\sigma_{\mathrm{B}}^2 = \sigma_{\mathrm{U}}^2 = 0.2$.

the probability that angle difference $\phi_{0\mathrm{p}}$ is small increases, which in turn increases the opportunity for enabling NOMA and reduces the negative effect of beam misalignment. Hence, the coverage probabilities of user U_0 in the proposed NOMA scheme and user U_{p} in all considered schemes increase with λ. On the other hand, the coverage probabilities of user U_0 in conventional NOMA and OMA do not depend on λ, as the probability that user U_0 is served by using NOMA is independent of λ. Because of the higher probability that NOMA is enabled, the coverage probabilities of both users are higher for the proposed NOMA scheme with angle-based user pairing compared to conventional NOMA with distance-based user pairing.

Fig. 5 shows the impact of the target data rate of the paired NOMA user on the sum rate. As R_{p} increases, the sum rates of all considered schemes improve. However, because the coverage probability of user U_{p} decreases with R_{p}, the rate of improvement of the sum rate decreases for large R_{p}. Moreover, we observe that the sum rate gap between NOMA and OMA becomes larger when R_{p} increases, which indicates that the sum rate gain of NOMA over OMA is higher when the paired NOMA users have more diverse target data rates. This is because the SINR requirements for OMA to achieve the same spectral efficiency as NOMA increase disproportionally for large R_{p}. The proposed NOMA scheme achieves a higher sum rate than conventional NOMA as both NOMA users are more likely able to exploit the array gain. In fact, for $R_{\mathrm{p}} = 4$ BPCU, conventional NOMA performs even worse than OMA

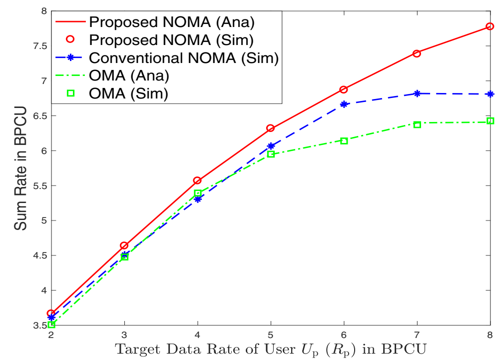

Fig. 5: Sum rate versus target data rate of user U_{p} when $P_{\mathrm{B}} = 0$ dBm, $\lambda = 0.0002$ nodes/m^2, and $\sigma_{\mathrm{B}}^2 = \sigma_{\mathrm{U}}^2 = 0.2$.

since it is more severely affected by beam misalignment.

V. Conclusions

In this paper, we developed a general performance analysis framework for mmWave-NOMA networks with spatially random users. The proposed framework takes into account link blockage, directional beamforming, beam misalignment, and user pairing. To facilitate NOMA transmission in mmWave networks, we proposed an angle-based user pairing strategy. Tools from stochastic geometry were utilized to derive the coverage probability and the sum rate. Simulation results demonstrated the performance gains of the proposed NOMA scheme over conventional NOMA with distance-based user pairing and OMA in mmWave networks, especially when the difference between the target data rates of the paired NOMA users is high.

Appendix

A. Proof of Lemma 1

As the spatial locations of the LOS users form an inhomogeneous PPP Φ_{L} with density $\lambda p(r)$, the CDF of the distance between the base station and a randomly selected LOS user is

$$F_{\mathrm{L}}(r) = \frac{\int_0^r p(x)x\mathrm{d}x}{\int_0^R p(x)x\mathrm{d}x} \overset{(a)}{=} \frac{1}{\rho}\int_0^r \exp\left(-\frac{x}{\eta}\right)x\mathrm{d}x, \tag{29}$$

where (a) follows by substituting $p(x) = \exp(-\frac{x}{\eta})$ and defining $\rho = \int_0^R \exp(-\frac{x}{\eta})x\mathrm{d}x = \eta^2\left(1 - \exp\left(-\frac{R}{\eta}\right)\left(1 + \frac{R}{\eta}\right)\right)$. By taking the first derivative of $F_{\mathrm{L}}(r)$ in (29), we obtain the PDF of the distance between the base station and a randomly selected LOS user given in (10). Following similar steps, we obtain the PDF of the distance of a randomly selected NLOS user given in (11).

B. Proof of Lemma 2

Although the spatial locations of the LOS users follow an inhomogeneous PPP Φ_{L}, the spatial distribution of the LOS users is isotropic. As angle ϕ_i is uniformly distributed within $[0, 2\pi]$ and is independent of angle $\phi_j, j \neq i$, the CDF of $\phi_{0i} = |\phi_0 - \phi_i|$ is $F_{\phi_{0i}}(\phi) = \frac{4\pi\phi - \phi^2}{4\pi^2}, \phi \in [0, 2\pi]$. By taking the first derivative of $F_{\phi_{0i}}(\phi)$, the PDF of ϕ_{0i} is given by $f_{\phi_{0i}}(\phi) = \frac{\mathrm{d}}{\mathrm{d}\phi}F_{\phi_{0i}}(\phi) = \frac{2\pi - \phi}{2\pi^2}, \phi \in [0, 2\pi]$. When there are k_{L} LOS users and user U_0 is LOS, the CDF of angle difference

$\phi_{0\mathrm{p}}$ is $F_{\phi_{0\mathrm{p}}}(\phi) \overset{(a)}{=} 1-\left(\frac{2\pi-\phi}{2\pi}\right)^{2k_{\mathrm{L}}-2}$, where (a) follows from the user pairing strategy in (2) and by applying order statistics [19]. When there are k_{L} LOS users and user U_0 is NLOS, by following similar steps, we obtain the CDF of angle difference $\phi_{0\mathrm{p}}$ as $F_{\phi_{0\mathrm{p}}}(\phi)=1-\left(\frac{2\pi-\phi}{2\pi}\right)^{2k_{\mathrm{L}}}$. By taking the first derivative of $F_{\phi_{0\mathrm{p}}}(\phi)$, we obtain the PDF of $\phi_{0\mathrm{p}}$ in (14).

C. Proof of Lemma 3

When the angle difference $\phi_{0\mathrm{p}}$ is given, the typical user is covered by the main lobe of the base station if $|\frac{1}{2}\phi_{0\mathrm{p}}+\Delta_{\mathrm{B}}| \leq \frac{1}{2}\Theta_{\mathrm{B}}^{\mathrm{NOMA}}$, which can equivalently be expressed as $\Delta_{\mathrm{B}} \in \left[-\frac{1}{2}\left(\Theta_{\mathrm{B}}^{\mathrm{NOMA}}+\phi_{0\mathrm{p}}\right), \frac{1}{2}\left(\Theta_{\mathrm{B}}^{\mathrm{NOMA}}-\phi_{0\mathrm{p}}\right)\right]$. As beamsteering error Δ_{B} is assumed to follow a Gaussian distribution, the probabilities that user U_0 is covered by the main lobe and the side lobe of the base station can be expressed as $g(\phi_{0\mathrm{p}}) = F_{\Delta_{\mathrm{B}}}\left(\frac{\Theta_{\mathrm{B}}^{\mathrm{NOMA}}-\phi_{0\mathrm{p}}}{2}\right)-F_{\Delta_{\mathrm{B}}}\left(-\frac{\Theta_{\mathrm{B}}^{\mathrm{NOMA}}+\phi_{0\mathrm{p}}}{2}\right)$ and $1-g(\phi_{0\mathrm{p}})$, respectively. The base station is covered by the main lobe of user U_0 if the beamsteering error $\Delta_{\mathrm{U}_0} \in \left[-\frac{1}{2}\Theta_{\mathrm{U}}, \frac{1}{2}\Theta_{\mathrm{U}}\right]$. Hence, the probability that the base station is covered by the main lobe and the side lobe of the typical user can be expressed as $y=F_{\Delta_{\mathrm{U}}}\left(\frac{1}{2}\Theta_{\mathrm{U}}\right)-F_{\Delta_{\mathrm{U}}}\left(-\frac{1}{2}\Theta_{\mathrm{U}}\right)$ and $1-y$, respectively.

As $\mathcal{D}_0^{\mathrm{NOMA}} = G_{\mathrm{B}}\left(\Theta_{\mathrm{B}}^{\mathrm{NOMA}}, \frac{1}{2}\phi_{0\mathrm{p}}+\Delta_{\mathrm{B}}\right) G_{\mathrm{U}}\left(\Theta_{\mathrm{U}}, \Delta_{\mathrm{U}_0}\right)$, the PMF of the total directivity gain between the base station and the typical user when NOMA is enabled is given by

$$\mathbb{P}\left(\mathcal{D}_0^{\mathrm{NOMA}}=z\right)=\sum_{x\in\Lambda}\mathbb{P}\left(G_{\mathrm{B}}\left(\Theta_{\mathrm{B}}^{\mathrm{NOMA}}, \frac{1}{2}\phi_{0\mathrm{p}}+\Delta_{\mathrm{B}}\right)=x\right) \times \mathbb{P}\left(G_{\mathrm{U}}\left(\Theta_{\mathrm{U}}, \Delta_{\mathrm{U}_0}\right)=\frac{z}{x}\right), \tag{30}$$

where $\Lambda=\left\{G_{\mathrm{B}}^{\mathrm{M}}\left(\Theta_{\mathrm{B}}^{\mathrm{NOMA}}\right), G_{\mathrm{B}}^{\mathrm{S}}\left(\Theta_{\mathrm{B}}^{\mathrm{NOMA}}\right)\right\}$.

As a result, we obtain the PMF of the total directivity gain D_0^{NOMA} given in (15). Following similar steps, we obtain the PMF of the total directivity gain $D_{\mathrm{p}}^{\mathrm{NOMA}}$ given in (16).

D. Proof of Proposition 1

With k_{L} LOS users and k_{N} NLOS users, $Q_{0,\mathrm{L}}$ is given by $Q_{0,\mathrm{L}}=\int_0^{\Theta_{\mathrm{B}}^{\mathrm{NOMA}}}\mathbb{P}\left(\gamma_{0|\mathrm{p}}\geq T_0\right) f_{\phi_{0\mathrm{p}}}(\phi_{0\mathrm{p}})\mathrm{d}\phi_{0\mathrm{p}}$.

Given the angle difference $\phi_{0\mathrm{p}}$, we have

$$\mathbb{P}\left(\gamma_{0|\mathrm{p}}\geq T_0\right) \overset{(a)}{=} \mathbb{P}\left(|h_0|^2 \geq \frac{\xi_1}{\mathcal{D}_0^{\mathrm{NOMA}}\ell_{\mathrm{L}}(r_0)}\right) \overset{(b)}{=} \sum_{n=0}^{N_{\mathrm{L}}-1}\frac{(N_{\mathrm{L}}\xi_1)^n}{n!}\mathbb{E}_{\left\{\mathcal{D}_0^{\mathrm{NOMA}},r_0\right\}}\left[\frac{\exp\left(-\frac{N_{\mathrm{L}}\xi_1}{\mathcal{D}_0^{\mathrm{NOMA}}\ell_{\mathrm{L}}(r_0)}\right)}{\left(\mathcal{D}_0^{\mathrm{NOMA}}\ell_{\mathrm{L}}\left(r_0\right)\right)^n}\right], \tag{31}$$

where (a) follows by substituting (3) and by defining $\xi_1 = \frac{T_0\sigma^2}{\left(\alpha_0^2-T_0\alpha_{\mathrm{p}}^2\right)P_{\mathrm{B}}}$, and (b) follows from the normalized Gamma distribution of $|h_0|^2$. Note that $\mathbb{E}_{\left\{\mathcal{D}_0^{\mathrm{NOMA}},r_0\right\}}[\cdot]$ is the expectation over the total directivity gain $\mathcal{D}_0^{\mathrm{NOMA}}$ and distance r_0.

By utilizing the PMF of the total directivity gain $\mathcal{D}_0^{\mathrm{NOMA}}$ given in Lemma 3, we have

$$\mathbb{E}_{\left\{\mathcal{D}_0^{\mathrm{NOMA}},r_0\right\}}\left[\frac{\exp\left(-\frac{N_{\mathrm{L}}\xi_1}{\mathcal{D}_0^{\mathrm{NOMA}}\ell_{\mathrm{L}}(r_0)}\right)}{\left(\mathcal{D}_0^{\mathrm{NOMA}}\ell_{\mathrm{L}}\left(r_0\right)\right)^n}\right] \overset{(a)}{=} \mathbb{E}_{\{r_0\}}\left[\sum_{i=1}^{4}\frac{d_i(\phi_{0\mathrm{p}})}{\left(c_i\ell_{\mathrm{L}}(r_0)\right)^n}\exp\left(-\frac{N_{\mathrm{L}}\xi_1}{c_i\ell_{\mathrm{L}}(r_0)}\right)\right] \overset{(b)}{=} \sum_{i=1}^{4}d_i(\phi_{0\mathrm{p}})\int_0^R\left(\frac{r_0^{\beta_{\mathrm{L}}}}{c_iC_{\mathrm{L}}}\right)^n\exp\left(-\frac{N_{\mathrm{L}}\xi_1 r_0^{\beta_{\mathrm{L}}}}{c_iC_{\mathrm{L}}}\right)f_{\mathrm{L}}(r_0)\mathrm{d}r_0, \tag{32}$$

where (a) and (b) follow by taking the expectations over $\mathcal{D}_0^{\mathrm{NOMA}}$ and r_0, respectively. By substituting (32) into (31), we obtain $Q_{0,\mathrm{L}}$ given in (18). By following similar steps and considering the PMF of the total directivity gain $\mathcal{D}_{\mathrm{p}}^{\mathrm{NOMA}}$ given in (16), we obtain $Q_{\mathrm{p},\mathrm{L}}$ given in (19).

References

[1] V.W.S. Wong, R. Schober, D.W.K. Ng, and L. C. Wang, *Key Technologies for 5G Wireless Systems*. Cambridge University Press, 2017.

[2] Y. Saito, A. Benjebbour, Y. Kishiyama, and T. Nakamura, "System-level performance evaluation of downlink non-orthogonal multiple access (NOMA)," in *Proc. of IEEE PIMRC*, London, UK, Sept. 2013.

[3] Y. Sun, D. W. K. Ng, Z. Ding, and R. Schober, "Optimal joint power and subcarrier allocation for full-duplex multicarrier non-orthogonal multiple access systems," *IEEE Trans. Commun.*, vol. 65, no. 3, pp. 1077–1091, Mar. 2017.

[4] Z. Ding, P. Fan, and V. Poor, "Impact of user pairing on 5G non-orthogonal multiple access downlink transmissions," *IEEE Trans. Veh. Technol.*, vol. 65, no. 8, pp. 6010–6023, Sept. 2016.

[5] Y. Zhou and V. W.S. Wong, "Stable throughput region of downlink NOMA transmissions with limited CSI," in *Proc. of IEEE ICC*, Paris, France, May 2017.

[6] Y. Zhou, V. W.S. Wong, and R. Schober, "Performance analysis of cooperative NOMA with dynamic decode-and-forward relaying," in *Proc. of IEEE Globecom*, Singapore, Dec. 2017.

[7] W. Roh, J.-Y. Seol, J. Park, B. Lee, J. Lee, Y. Kim, J. Cho, K. Cheun, and F. Aryanfar, "Millimeter-wave beamforming as an enabling technology for 5G cellular communications: Theoretical feasibility and prototype results," *IEEE Commun. Mag.*, vol. 52, no. 2, pp. 106–113, Feb. 2014.

[8] 3GPP TR 36.873, "Technical specification group radio access network: Study on 3D channel model for LTE," Sept. 2017.

[9] T. Bai and R. W. Heath, "Coverage and rate analysis for millimeter-wave cellular networks," *IEEE Trans. Wireless Commun.*, vol. 14, no. 2, pp. 1100–1114, Feb. 2015.

[10] Z. Ding, P. Fan, and H. Poor, "Random beamforming in millimeter-wave NOMA networks," *IEEE Access*, vol. 5, pp. 7667–7681, Feb. 2017.

[11] Z. Ding, L. Dai, R. Schober, and H. V. Poor, "NOMA meets finite resolution analog beamforming in massive MIMO and millimeter-wave networks," *IEEE Commun. Lett.*, no. 8, pp. 1879–1882, Aug. 2017.

[12] D. Zhang, Z. Zhou, C. Xu, Y. Zhang, J. Rodriguez, and T. Sato, "Capacity analysis of NOMA with mmWave massive MIMO systems," *IEEE J. Sel. Areas Commun.*, vol. 35, no. 7, pp. 1606–1618, Jul. 2017.

[13] J. Wildman, P. H. J. Nardelli, M. Latva-aho, and S. Weber, "On the joint impact of beamwidth and orientation error on throughput in directional wireless Poisson networks," *IEEE Trans. Wireless Commun.*, vol. 13, no. 12, pp. 7072–7085, Dec. 2014.

[14] M. R. Akdeniz, Y. Liu, M. K. Samimi, S. Sun, S. Rangan, T. S. Rappaport, and E. Erkip, "Millimeter wave channel modeling and cellular capacity evaluation," *IEEE J Sel. Areas Commun.*, vol. 32, no. 6, pp. 1164–1179, Jun. 2014.

[15] J. G. Andrews, T. Bai, M. N. Kulkarni, A. Alkhateeb, A. K. Gupta, and R. W. Heath, "Modeling and analyzing millimeter wave cellular systems," *IEEE Trans. Commun.*, vol. 65, no. 1, pp. 403–430, Jan. 2017.

[16] A. Alkhateeb, Y.-H. Nam, M. S. Rahman, J. Zhang, and R. W. Heath, "Initial beam association in millimeter wave cellular systems: Analysis and design insights," *IEEE Trans. Wireless Commun.*, vol. 16, no. 5, pp. 2807–2821, May 2017.

[17] 3GPP TR 36.859, "Study on downlink multiuser superposition transmission (MUST) for LTE," Jan. 2016.

[18] Y. Liu, Z. Ding, M. Elkashlan, and H. V. Poor, "Cooperative non-orthogonal multiple access with simultaneous wireless information and power transfer," *IEEE J. Sel. Areas Commun.*, vol. 34, no. 4, pp. 938–953, Apr. 2016.

[19] H. A. David and H. N. Nagaraja, *Order Statistics*. John Wiley, New York, 2003.